Experimental Investigation and Numerical Simulation on Surge in a Low-Specific-Speed Centrifugal Blower

Hassan, Ahmed Sayed Ahmed
Graduate school of Engineering Sciences Kyushu University

Hayami, Hiroshi
Institute of Advanced Material Study, Kyushu University

https://doi.org/10.15017/6680

出版情報：九州大学機能物質科学研究所報告. 9 (2), pp.155-166, 1996-03-28. 九州大学機能物質科学研究所
バージョン：
権利関係：

機能物質科学研究所
報告 第9巻 第2号
pp.155～166(1995)

Experimental Investigation and Numerical Simulation on Surge in a Low-Specific-Speed Centrifugal Blower

Ahmed Sayed Ahmed HASSAN*, and Hiroshi HAYAMI**

A low-specific-speed centrifugal blower with a low-solidity cascade diffuser was tested and the time variation of static pressure was measured at several locations on the side walls between cascade vanes, at the vaneless zone and at the blower intake using high frequency response pressure transducers. The time variation of flow rate was also measured at the blower intake using a hot-wire anemometer. Surge, and so called surge cycle, in the centrifugal blower were discussed based on the time histories of pressure and flow. In addition to the data analysis of the experiments, numerical simulation was made for the system dynamic model including the effect of B-parameter and the numerical results were compared with the experimental data.

1. Introduction

Surge is a phenomenon of interest, yet it is not fully understood. Especially, the understanding of this phenomenon in centrifugal compressors is considerably poorer than that in axial compressors. It is a kind of unstable operation and should be avoided in both design and operation. Surge is often symptomized by excessive vibration and an audible sound, and it is quite evident that the underlying cause of surge is aerodynamic stall.

Hayami et al.[1] experimentally investigated the effects of low-solidity cascade vanes and the cascade stagger angle on the initiation of stall and surge using a low-speed centrifugal blower. They concluded that the blower with cascade vanes fell in surge without falling in rotating stall owing to suppression of rotating stall by the cascade vanes. Also they concluded that the cascade stagger angle controlled stall and surge. In the present work the blower was tested at four values of B-parameter by changing impeller speed. In addition to the data analysis of the experiments, numerical simulation was made for the system dynamic model including the effect of B-parameter and the numerical results were compared with the experimental data.

2. Experimental Apparatus and Procedure

The general view of the experimental apparatus is shown in Fig.1. The test blower is a low specific speed type, 0.059 in non-dimensional specific speed. The diameter of the impeller was 500 mm and the exit blade height was 14 mm. The impeller had eighteen blades with inlet and exit angles of 66.5 deg and 41.5 deg from circumference respectively. At the exit

Received December 21, 1995
*Graduate school of Engineering Sciences, Kyushu University, Kasuga, Fukuoka, 816, Japan
**Institute of Advanced Material Study, Kyushu University, Kasuga, Fukuoka, 816, Japan

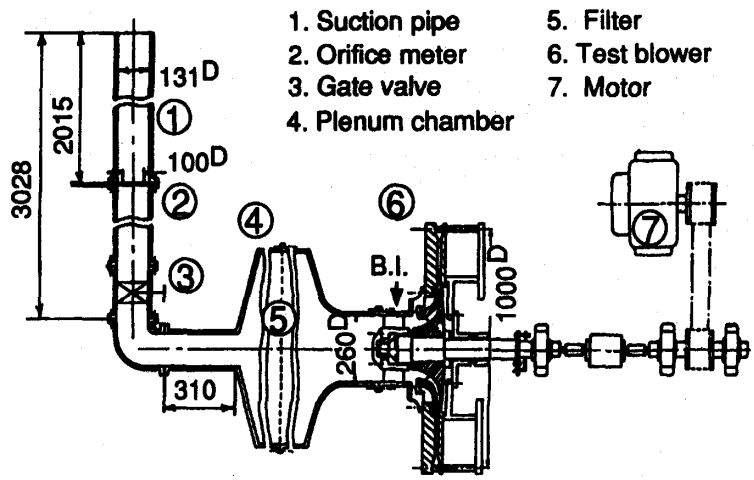

Fig. 1 General view of experimental apparatus

of impeller, there was a diffuser which consisted of two parallel walls 14 mm apart from each other and 1000 mm in diameter. The circular cascade was located between the two parallel walls. The leading edges of cascade vanes were 270 mm away from the axis. The cascade stagger angle was 70 deg and the solidity was 0.69 with eleven vanes. This cascade was identified as A1 type[2], which is shown in Fig.2. The exit of diffuser was opened to the atmosphere. The flow rate was controlled with a valve at the suction pipe and was measured with an orifice type flow meter in the pipe. The suction pipe was followed by a plenum chamber and air was accelerated to the intake of blower.

In addition to securing conventional blower characteristics, the time variation of static pressure was measured at 4 points in the cascade diffuser (D1 to D4 in Fig.2), and at the blower intake (B.I. in Fig.1) using pressure sensors with high frequency response (Kulite XT -190 with 150 kHz in natural frequency). The time variation of flow rate was measured using a hot wire anemometer located at the center line of the blower intake B.I., 235 mm upstream from the impeller inlet.

The measurement system of unsteady pressure and flow is shown in Fig.3. The impeller blade passing frequency was 600 Hz- 1050 Hz for eighteen blades at the impeller speed of 2000 rpm- 3500 rpm. The pressure signals and the signal from the hot wire were sampled simultaneously for 1 s at 20 kHz in sampling rate and digitized through an A/D convertor board with a function of simultaneous sampling (CANOPUS ADXM-LB1S) installed in a personal computer (NEC PC9801AP2), and the final data were recorded in MO disk. All signals from pressure transducers were amplified by 400-1000 times through a DC amplifier (Unipulse AM30AZ), and they were processed using a low-pass filter of 10 kHz in cut-off frequency. The wave analysing software DaDISP (V.3.01) was applied for data analysis.

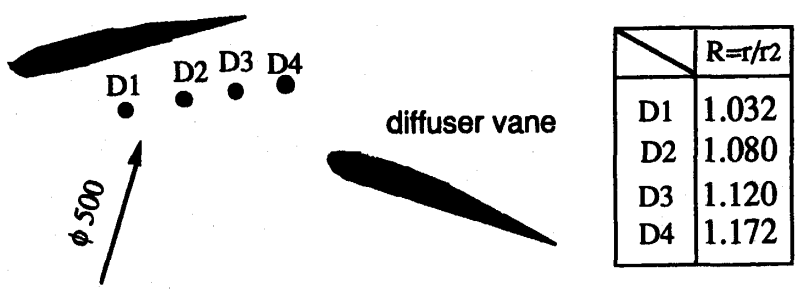

	R=r/r2
D1	1.032
D2	1.080
D3	1.120
D4	1.172

Fig. 2 Locations of pressure transducer, A1 cascade

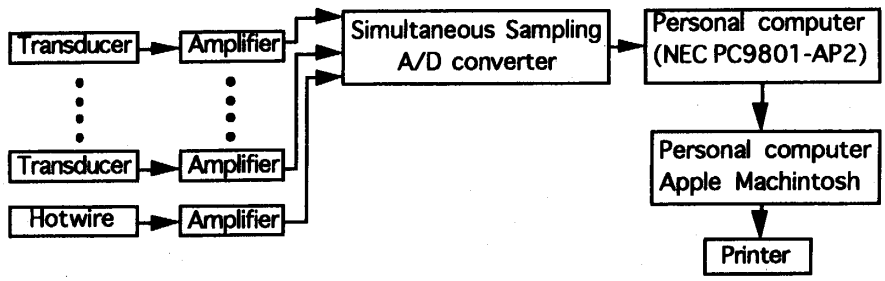

Fig. 3 Measurement system of unsteady pressure and flow rate

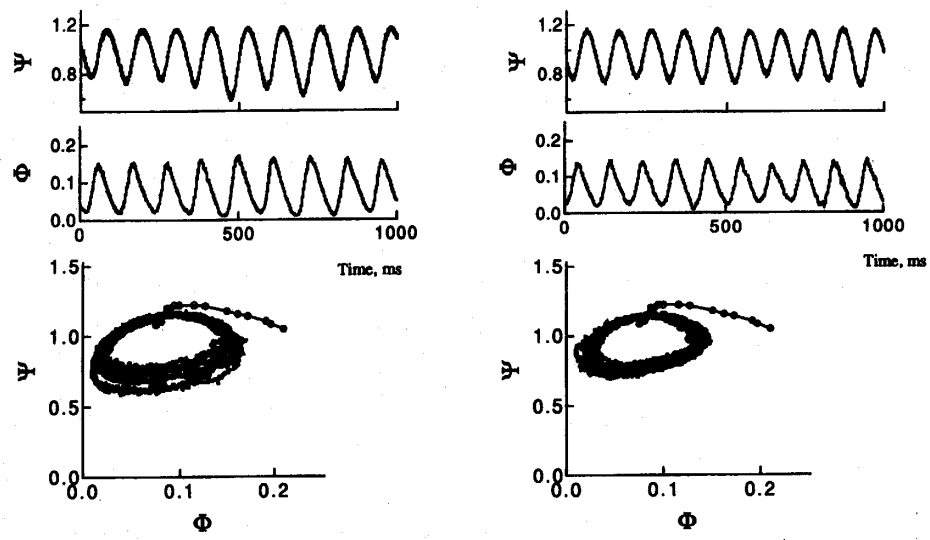

(a) N=3500 rpm **(b) N=3000 rpm**

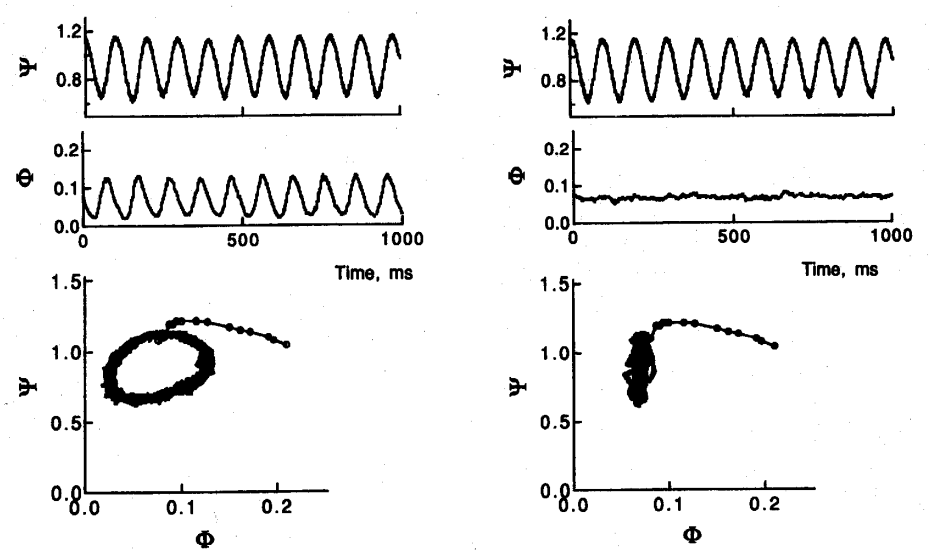

(c) N=2500 rpm **(d) N=2000 rpm**

Fig. 4 Experimental system response, different impeller speed, $\bar{\Phi}=0.081$

3. Effect of B-Parameter on Surge Initiation

The blower was tested with four values of B-parameter by changing impeller speed of, 3500, 3000, 2500, and 2000 rpm. The upper two figures in Figs.4(a)-4(d) represent the time history of nondimensional pressure Ψ and flow coefficient Φ respectively, for time-mean flow coefficient of, $\bar{\Phi}=0.081$. The pressure coefficient Ψ is also plotted against the flow coefficient Φ in the lower part of Figs.4(a)-4(d). It is seen that the amplitude of flow fluctuation decreased as the impeller speed or B-parameter decreased, while that of pressure fluctuation remained relatively constant. These results for the low-specific-speed centrifugal blower agree well with the results for the axial compressors[3].

Power spectra (PSD) and root mean square (RMS) of pressure fluctuation at the blower intake are represented in Figs.5 and 6 respectively for various flow rates. At $\bar{\Phi}=0.088$, a low frequency component of about 8 Hz was predominant at all speeds. The level of PSD at this flow rate was rather low in comparison with that of lower flow rate but this is one of the trigger for surge as defined for the identical test blower. The level of PSD increased as flow rate decreased keeping the same predominant frequency of about 8 Hz. The level of RMS of the pressure fluctuation increased as the impeller speed increased.

The normalized RMS of flow fluctuation Φrms by the impeller tip speed U and the normalized RMS of static pressure fluctuations Ψrms by $0.5\rho U^2$ are represented against the time-mean flow coefficient $\bar{\Phi}$ in Figs.7 and 8 respectively. At $\bar{\Phi}=0.088$, Φrms was the same at all impeller speeds. When the flow rate decreased, however, the RMS of flow rate fluctuation became higher depending on impeller speed. In contrast, when the pressure fluctuations of Fig.6 were nondimensionalized as shown in Fig.8, the RMS of static pressure fluctuations Ψrms increased with decrease in flow rate but approximately independent to impeller speed. These results agree well with the data reported by Greitzer[3] and Abdel-Hamid et al.[4].

The power spectra of nondimensional pressure fluctuations at vaneless space region (D1), at cascade inlet (D2), at between cascade vanes (D3) and at cascade throat (D4) for the impeller speeds of 3500, 3000, 2500, and 2000 rpm are represented in Figs.9(a-d) respectively. The blower was tested at five different flow rates. At flow, $\bar{\Phi}=0.089$, the impeller

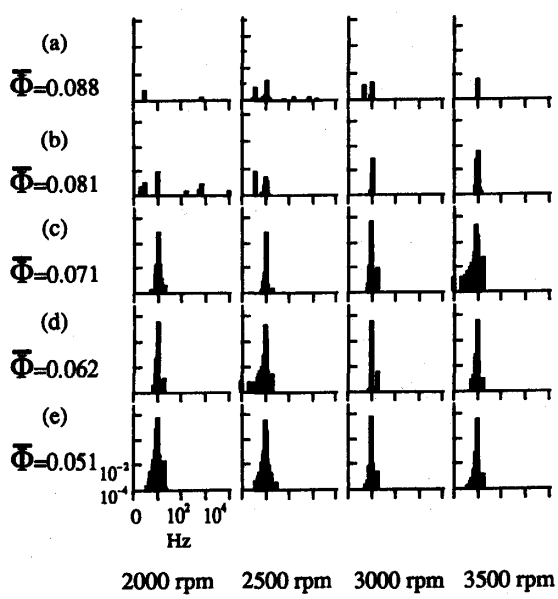

Fig. 5 Power spectrum at blower intake

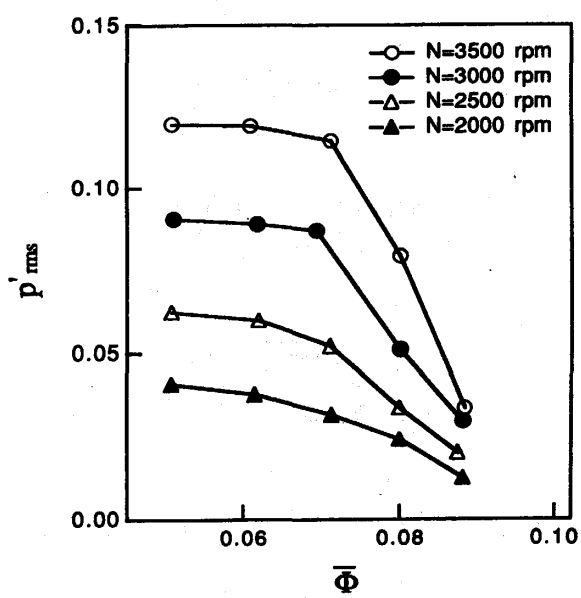

Fig. 6 RMS of pressure fluctuation at blower intake

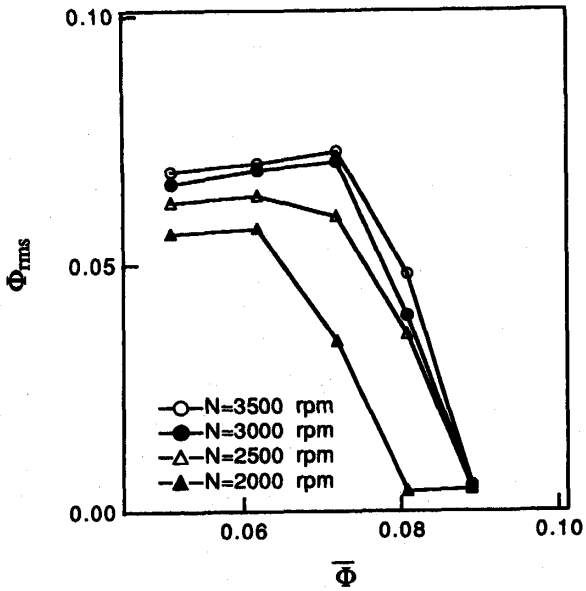

Fig. 7 RMS of flow fluctuations

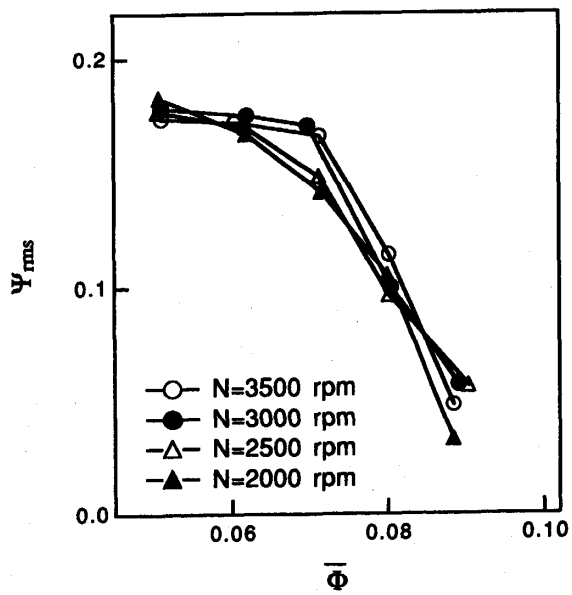

Fig. 8 RMS of pressure coefficient at blower intake

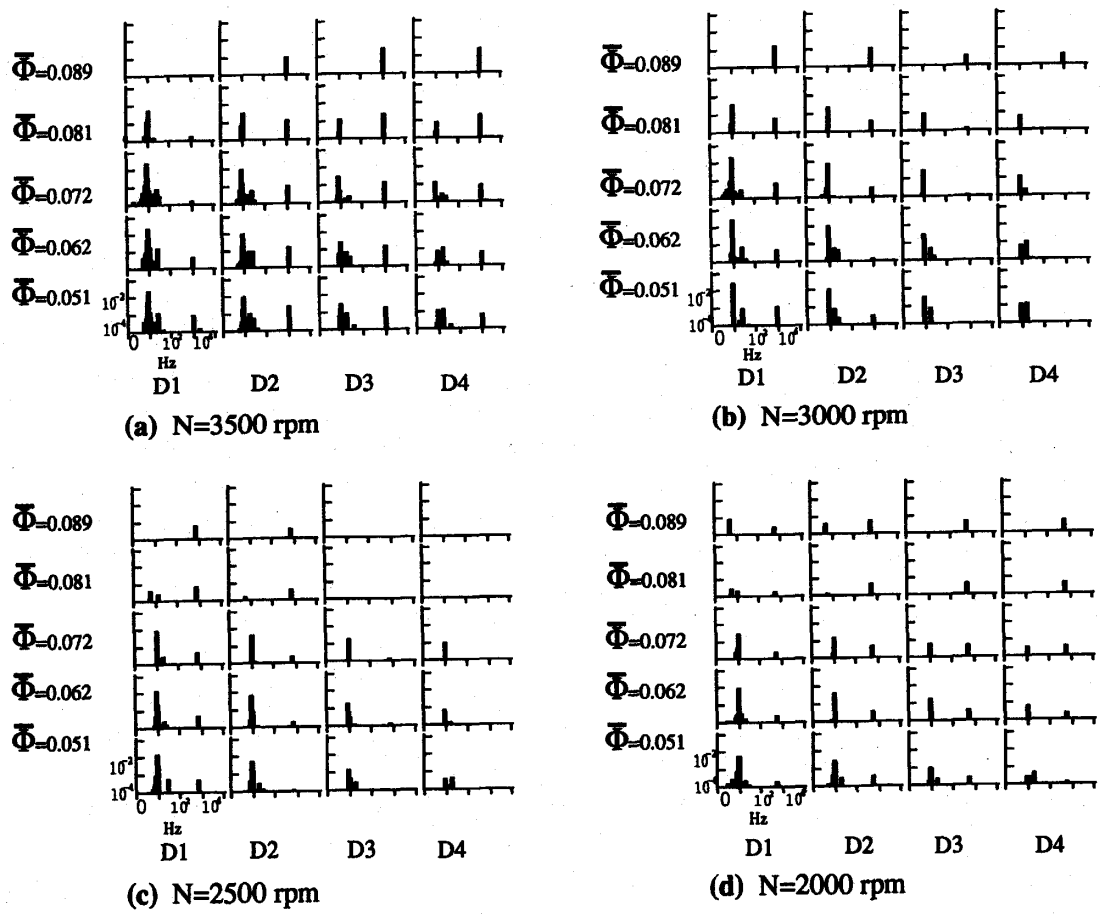

Fig. 9 Power spectrum, different speeds

blade passing frequency component of 1050 Hz, 900 Hz, and 750 Hz due to the passing of the impeller blades was predominant at the higher speeds of 3500 rpm, 3000 rpm, and 2500 rpm respectively, and no indication for surge initiation was observed in the PSD at higher speed patterns. But, at the lower impeller speed of 2000 rpm, the same frequency of surge with a frequency component of 8 Hz appeared at the cascade inlet as shown in Fig.9d. At $\bar{\Phi}=0.081$, on the other hand, the level of PSD of about 8 Hz was completely decayed between cascade vanes. Further decreasing flow rate results an increase in the amplitude of pressure fluctuations with the same frequency. For any speed condition, the amplitude of pressure fluctuation decayed through D1 to D4, and the same surge frequency of 8 Hz was observed. That is, the rotor speed has no effect on surge initiation substantially at least in the present test range. On the other hand, the level of PSD due to the interaction between the rotating impeller blades and diffuser cascade gradually decreased as the impeller speed decreased.

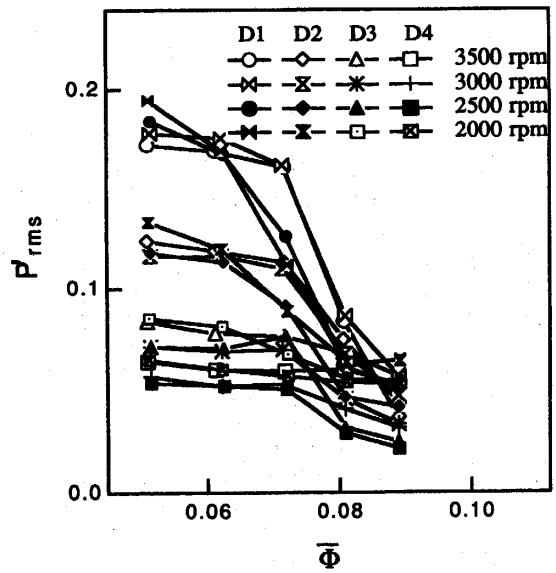

Fig. 10 RMS of static pressure fluctuations

The RMS of nondimensional pressure fluctuations are shown in Fig.10. The RMS of pressure fluctuation decayed through D1 to D4 since the outlet of the diffuser was opened to the atmosphere, and it was more significant at low flow rate. The effect of impeller speed is more complicated than that we discussed above. That is, at D1, the steep gradient position of P'rms against $\bar{\Phi}$ varied with the impeller speed. Then, it may be supposed that the initiation of surge delayed a little bit at lower impeller speed.

4. Numerical Solution and Comparison with the Experimental Results

Greitzer[5] proposed that the dynamics of surge behavior in axial compressors is controlled by the magnitude of B-parameter. When this parameter exceeds a certain value, the onset of rotating stall will trigger the global instability of surge. Since B is a system parameter which is a measure of the ratio of system compliance to inductance, its influence on overall system behavior is independent of compressor type. Hence the overall surge behavior of a centrifugal compressor would also depend on this parameter. In the present work, the system dynamic model including the effect of B-parameter is discussed.

4.1 Assumptions

In order to examine numerically the system response with the different system elements, i.e. with different value of non-dimensional parameter$B$, the followings are assumed:

1- The duct area is constant and is referred to the area of blower intake pipe.
2- The gas angular momentum in the blower passages is negligible compared to the impeller angular momentum.
3- The fluid inertia in the throttle is negligible.
4- The blower follows a quasi-steady characteristic.
5- The flow in the inlet ducting is one-dimensional, incompressible and inviscid.
6- The plenum processes are isentropic.

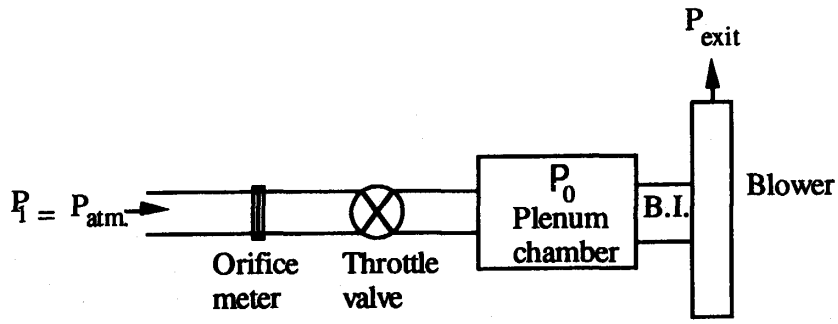

Fig. 11 System model

7- Velocity in the plenum chamber is negligible.
8- The rotor speed is allowed to vary, and accordingly the B-parameter becomes a time dependent variable to be calculated along with blower flow and pressure coefficient.

4.2 System Modeling and Governing Equations

The basic elements of the blower system model considered in the present work are identical to those considered by Greitzer[3] and by Fink[5,6]. As shown in Fig.11 the model is composed of a long inlet pipe, a throttle valve, a plenum chamber, a blower intake pipe, and a blower which is opened to the atmosphere. The governing equations describing the unsteady behavior of the system model are the conservation of momentum in the inlet pipe, the conservation of mass in the plenum chamber, and the conservation of angular momentum in the blower.

The momentum equation for the blower inlet pipe is written as

$$L_b\frac{d}{dt}(\rho Cx)=(\Delta P_b-\Delta P) \tag{1}$$

where L_b is the length of blower intake pipe, Cx is the axial velocity at blower intake pipe, $\Delta P(=P_{exit}-P_0)$ is the plenum pressure, and ΔP_b is the blower pressure rise. In terms of blower mass flow, this can be written as

$$L_b\frac{d}{dt}(\dot{m})=(\Delta P_b-\Delta P)A_b \tag{2}$$

The throttle and compressor mass flows are linked by mass conservation in the plenum

$$\dot{m}_t-\dot{m}=V_0\frac{d\rho_0}{dt} \tag{3}$$

where V_0 is the volume of plenum chamber. Using the isentropic relation, Eq.(3) becomes

$$\dot{m}_t-\dot{m}=\frac{V_0}{a^2}\frac{d\rho_0}{dt} \tag{4}$$

where a is the velocity of sound in the plenum chamber.

Equations (2) and (4) can be expressed non-dimensionally by the use of the followings: mass flows by $\rho A_D U$, the pressure differences by $0.5\rho U^2$, and the time using inverse Helmholtz angular frequency $1/(2\pi f_H)$, where f_H is the Helmholtz frequency in cycles per second. In addition, the non-dimensional stability parameter, B, was defined as

$$B=\frac{U}{2\omega_H L_b}=\frac{U}{2a}\sqrt{\frac{V_0}{A_b L_b}}$$

Employing this non-dimensionalization, Eqs.(2) and (4) can be written as

$$\frac{d}{dt}(B^*\Phi)=B^{*2}(\Psi_b-\Psi) \tag{5}$$

$$\Phi_t-\Phi=\frac{1}{B^*}\frac{d}{dt}(-\Psi B^{*2}) \tag{6}$$

where Ψ and Ψ_b are the non-dimensional blower pressure coefficient, and compressor pressure coefficient, respectively, and $B^*=B(A_b/A_D)$, where A_D is the area at the impeller exit.

Similarly, the equation for conservation of angular momentum in the blower system is given by

$$I\frac{d\omega}{dt}=T_d-T_b=T_{net}=I\frac{2\omega_H L_b}{r_2}\frac{dB}{dt} \tag{7}$$

where T_d and T_b are the drive torque and blower torque, respectively, T_{net} is the net torque, and ω is the impeller angular velocity. The net torque was non-dimensionalize using the quantity $\rho A_b r_2 U^2$, and denoted as J. Based on the impeller inertia I, the parameter H is defined as

$$H=\frac{2\rho_0 L_b A_b r^2_2}{I}\frac{A_D}{A_b} \tag{8}$$

Then, Eq. (7) can be written as

$$\frac{dB^*}{dT}=HJB^{*2} \tag{9}$$

Substituting Eq.(8) into Eqs.(5) and (6), then

$$\frac{d\Phi}{dT}=B^*\Psi_b-B^*\Psi-HJB^*\Phi \tag{9}$$

and

$$\frac{d\Psi}{dT}=\frac{1}{B^*}(\Phi-\Phi_t)-2HJB^*\Psi \tag{10}$$

4.3 Blower Characteristic

It is well known that the compression system is stable if the operation point is on the compressor characteristic curve with the negative slope and the system is unstable if the slope of the compressor characteristic is algebraically larger than that of the throttle characteristic. To determine the transient behavior of the system model shown in Fig.11, the non-linear equations, Eqs.(8), (9) and (10), are solved numerically for Ψ, Φ, and B^*, with the specifications such as the specified blower pressure coefficient $\Psi=f(\bar{\Phi})$, compressor pressure coefficient $\Psi_b=f(\bar{\Phi})$, and torque characteristics $J=f(\bar{\Phi})$, respectively. In steady state operation the pressure coefficient, $\Psi=f(\bar{\Phi})$ produced by the blower is a characteristic function of the mass flow rate. The experimental results are shown in Fig.12, together with an approximate empirical curve fit.

$$\Psi=0.085\ \arctan\ (120\,(\bar{\Phi}-0.082))+1.185+0.1\bar{\Phi}-6.3\bar{\Phi}^2-0.1\bar{\Phi}^3 \tag{11}$$

It is seen from the experimental results that the time mean value of the blower operating point at surge condition moved to a new operating point lower than the value at the manometric blower characteristic curve, therefore it is assumed that the compressor pressure coefficient in surge conditions also moved to a new operating point ($\bar{\Psi}_b$) at a value less than the manometric blower characteristic curve. The blower nondimensional net torque J is assumed as a function of the mass flow rate as

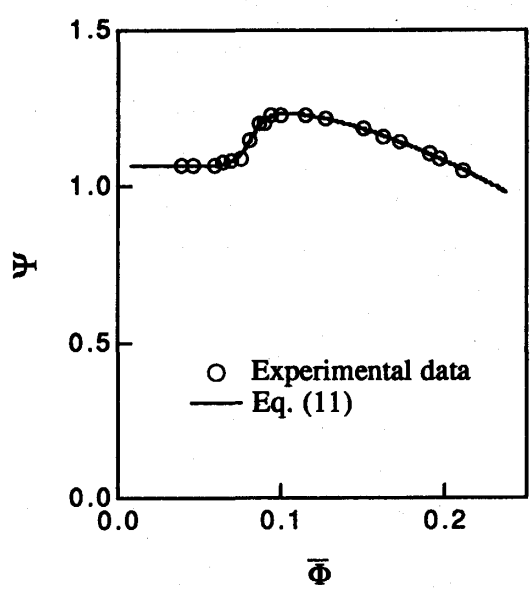

Fig. 12 Characteristic curve of the blower

a straight line relation, $J=C+C_1\bar{\Phi}$, where C is a constant representing the blower friction torque at zero flow rate, and C_1 is the slope of the net torque.

4.4 Numerical Solutions

To examine the system response, Eqs. (8)-(10) were solved numerically with a fourth order predictor-corrector method, the results are shown in Figs.13(a)-13(d) for different values of the parameter B^*, 0.260, 0.223, 0.186, and 0.149, respectively, at $\bar{\Phi}=0.081$. The Helmholtz frequency for the system in surge condition $\omega_H=50.3$ cycles/s was used based on the experimental result. Effect of B-parameter on the system behavior is clearly shown in this figure. The amplitude of flow fluctuations was decreased as the value B-parameter was

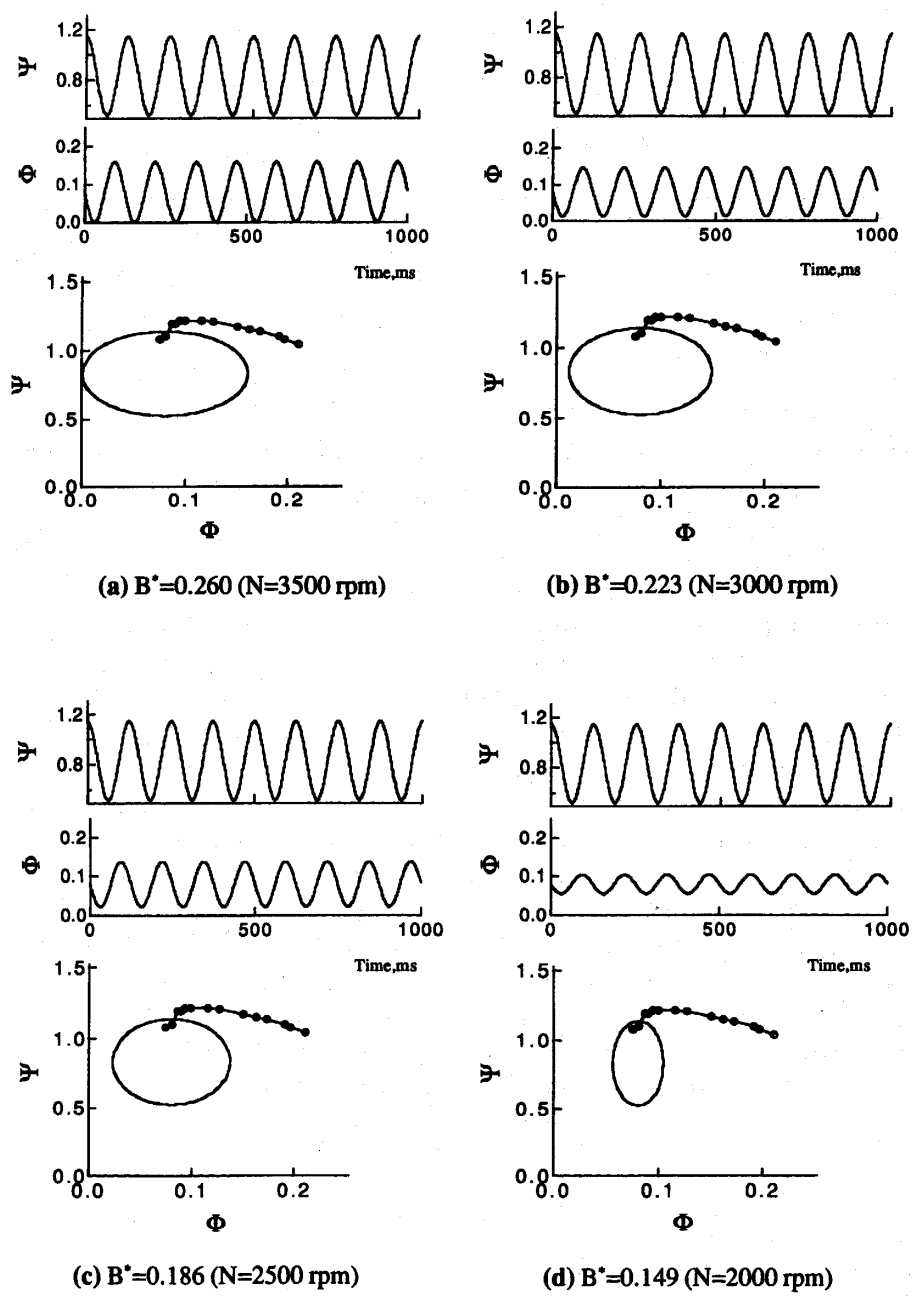

Fig. 13 Computed system response, effect of B-parameter

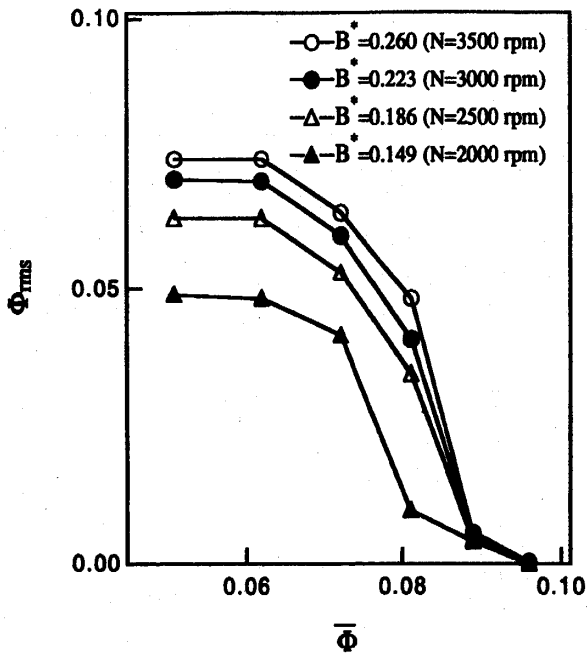

Fig. 14 RMS of flow fluctuations (Simulation)

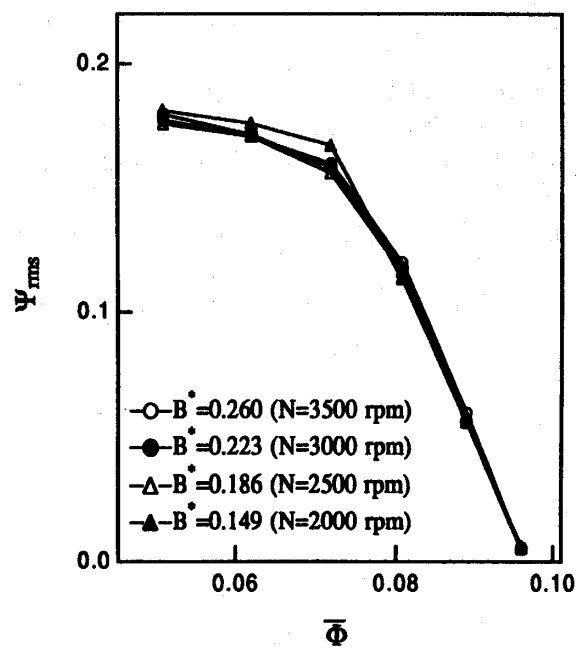

Fig. 15 RMS of pressure coefficient (Simulation)

decreased, while these in pressure coefficient remain relatively constant or even it may be a little increased. The time variations of the pressure coefficient, based on the system modeling at $B^*=0.260$, corresponding to rotor speed of 3500 rpm are shown in Figs.13(a).

The system response at a relatively low value of $B^*=$ 0.149, corresponding to the impeller speed of 2000 rpm, is shown Figs.13(d). A small amplitude of flow fluctuation was observed at the relatively low value of B^* in comparison with those at higher value of B-parameter, but the amplitude of pressure fluctuation remained relatively constant even with decrease in value of B-parameter. The width of the limit cycles becomes very small as the value of B-parameter was decreased and these results give a good agreement with the experimental results. The frequency of the waves of 8 Hz in Figs. 13(a)-13(d) did not change with decrease in B-parameter because the value of ω_H was used as a constant value of 50. 3 cycles/s with the different values of B^* of 0.260, 0.223, 0.186, and 0.149 for the comparison with the experimental results which have the same plenum volume.

Figures 14 and 15 show the effect of B-parameter on the RMS of flow fluctuation Φrms and the pressure fluctuation Ψrms. It is seen from these figures that as B-parameter was decreased the magnitude of flow fluctuations was decreased, but the amplitude of pressure fluctuations remained approximately constant. There is a large difference among the curves in Fig.14 due to the effect of decrease in B-parameter in surge conditions, but as clearly shown in Fig.15 there is no difference in the curves of pressure fluctuations inside the surge, and those can be compared directly with the experimental results of Figs.7 and 8 which have the same results and good agreement was obtained.

6. Conclusions

A centrifugal blower with a low-solidity cascade, 0.69 in solidity, 70 deg in stagger angle, was tested. Surge, and so called surge cycle in the centrifugal blower were discussed based on the time histories of pressure and flow. The initiation of surge does not change substantial-

ly even the impeller speed decreases. In addition to the data analysis of the experiments, numerical simulation was made for the system dynamic model including the effect of B-parameter. The numerical results were compared with the experimental data, and good agreement was obtained.

References

1) Hayami, H., Hassan, A.S.A., Hiraishi,E., and Hasegawa,H., "Experimental Investigation on Stall and Surge in centrifugal blower", Unsteady Aerodynamics and Aeroelasticity of Turbomachines, Elsevier (1995), 727.
2) Senoo, Y., Hayami, H., and Ueki, H., "Low-Solidity Tandem-Cascade Diffuser for Wide-Flow-Range Centrifugal Blower", ASME Paper No. 83-GT-3 (1983).
3) Greitzer, E.M., "Surge and Rotating Stall in Axial Flow Compressors", ASME Journal Engineering for Power, Vol. 98 (1976), 190.
4) Abdel-hamid, A.N., Colwill, J.F., and Barrows, J.F., "Experimental Investigation of Unsteady Phenomena in Vaneless Radial Diffuser", ASME Journal of Engineering for Power, Vol.101 (1979), 52.
5) Fink, D.A., Cumpsty, N.A., and Greitzer, E.M., "Surge Dynamics in a Free-Spool Centrifugal Compressor System" ASME Journal of Turbomachinery, Vol. 114 (1992), 321.
6) Fink, D.A., "Surge Dynamics and Unsteady Flow Phenomena in Centrifugal Compressors", MIT Gas Turbine Laboratory Report No.193 (1988).

Nomenclature

A_b =area of duct at blower intake
A_D =area at the impeller exit, $A_D=2\pi br_2$
a =velocity of sound
B =system non-dimensional parameter, $B=U/(2\omega_H L_b)$
b =width of diffuser or impeller exit
Cx =axial velocity at blower intake
f_H =Helmholtz frequency
G =mass flow rate
L_b =length of blower pipe
P_0 =pressure at plenum chamber
$P'rms$ = root mean square of static pressure fluctuation (non-dimensional), $P'rms=2p'rms/(\rho U^2)$
$p'rms$ = root mean square of static pressure fluctuation
R =radius ratio, $R=r/r_2$
r =radius
r_2 =radius of impeller
U =impeller tip speed
V_0 =volume of blower plenum
ρ =density
ρ_0 =density at plenum chamber
Φ =flow coefficient, $\Phi=G/(2\pi\rho br_2U)$
Φrms =root mean square of flow fluctuation
Ψ =pressure coefficient, $\Psi=2\Delta P/(\rho U^2)$
Ψrms =root mean square of pressure fluctuation
ω_H =Helmholtz angular frequency, $\omega_H=a(A_b/L_bV_0)^{0.5}=2\pi f_H$
Superscript

$\bar{}$ = time mean